SHN-1, a Shank homologue in *C. elegans*, affects defecation rhythm via the inositol-1,4,5-trisphosphate receptor

Changhoon Jee[a], Jungsoo Lee[a], Jin Il Lee[a], Won Hae Lee[a], Byung-Jae Park[a], Jae-Ran Yu[b], Eunhye Park[c], Eunjoon Kim[c], Joohong Ahnn[a,*]

[a] *Department of Life Science, Kwangju Institute of Science and Technology, Kwangju 500-712, South Korea*
[b] *Department of Parasitology, College of Medicine, Kon-Kuk University, Chungju 380-710, South Korea*
[c] *Creative Research Center for Synaptogenesis and Department of Biological Sciences KAIST, Kusong-dong, Daejon 305-701, South Korea*

Received 11 November 2003; revised 26 January 2004; accepted 26 January 2004

First published online 13 February 2004

Edited by Ned Mantei

Abstract Protein localization in the postsynaptic density (PSD) of neurons is mediated by scaffolding proteins such as PSD-95 and Shank, which ensure proper function of receptors at the membrane. The Shank family of scaffolding proteins contain PDZ (PSD-95, Dlg, and ZO-1) domains and have been implicated in the localizations of many receptor proteins including glutamate receptors in mammals. We have identified and characterized *shn-1*, the only homologue of Shank in *Caenorhabditis elegans*. The *shn-1* gene shows approximately 40% identity over 1000 amino acids to rat Shanks. SHN-1 protein is localized in various tissues including neurons, pharynx and intestine. RNAi suppression of SHN-1 did not cause lethality or developmental abnormality. However, suppression of SHN-1 in the *itr-1* (*sa73*) mutant, which has a defective inositol-1,4,5-trisphosphate (IP_3) receptor, resulted in animals with altered defecation rhythm. Our data suggest a possible role of SHN-1 in affecting function of IP_3 receptors in *C. elegans*.

Key words: Inositol-1,4,5-trisphosphate receptor; Postsynaptic density; Scaffolding protein; Receptor localization; Defecation cycle

1. Introduction

The correct localization of membrane proteins to distinct regions of cells is necessary for their proper function. Recently, protein scaffolding in the postsynaptic density (PSD) of mammalian neurons has been well studied. In particular the PDZ (PSD-95, Dlg, and ZO-1) domain links glutamate receptors with scaffolding proteins such as PSD-95/SAP90 and GRIP/ABP at the PSD [1–8].

The Shank/ProSAP/SSTRIP family of scaffolding proteins, which have PDZ domains, was originally isolated as a group of proteins that interact with the PSD-95/GKAP complex that is involved in the localization of glutamate receptors [9]. There are currently three members of the Shank family, Shank1, Shank2, and Shank3 [10]. All three proteins are relatively large, and the transcripts that encode these proteins are alternatively spliced during development [11–14]. Shank contains several domains including multiple ankyrin repeats near the N-terminus, an SH3 domain, a PDZ domain, a long proline-rich region, and a sterile alpha motif (SAM) domain at the C-terminus [9]. Rat Shank proteins are expressed mostly in the brain [11,15] and are highly enriched in the PSD of neurons [9]. Shank proteins have several binding partners in the PSD, including GKAP, the F-actin binding protein cortactin, and Homer, a multimodular protein [15,16]. Both cortactin and Homer bind to the proline-rich region of Shank. Cortactin is enriched in cell–matrix contact sites and lamellipodia of cultured cells as well as growth cones in neurons, and may play a regulatory role in the organization of the actin cytoskeleton both in cell cortex and in dendritic spines [15,17]. Homer is thought to play a general role in excitation–contraction coupling [8,10,18] and was shown to be involved in dendritic spine maturation by linking the inositol-1,4,5-trisphosphate (IP_3) receptor with Shank [19].

Though the wealth of information regarding biochemical interactions of Shank has elucidated its roles at the subcellular level, the lack of genetic information has hindered our understanding of Shank at the organism level. In this paper we have identified and characterized a homologue of Shank, *shn-1*, in *Caenorhabditis elegans*. We have shown that *shn-1* is expressed in neurons, pharynx, intestine, vulva, and sperm. Interestingly, RNA-mediated interference (RNAi) suppression of *shn-1* affected defecation rhythms in an IP_3 receptor mutant background, but not in wild-type animals. Our data suggest that there might be a genetic interaction between Shank and IP_3 receptors, which controls the defecation rhythm in *C. elegans*.

2. Materials and methods

2.1. Strains and culture conditions

Wild-type Bristol N2, *itr-1*(*sy290*)*IV*, *itr-1*(*sy331*)*IV*, *itr-1*(*sy328*)*IV* and *itr-1*(*sa73*)*IV* strains were obtained from the *C. elegans* Genetic Center (CGC). Strains *itr-1*(*sy290*)*IV*, *itr-1*(*sy331*)*IV*, *itr-1*(*sy328*)*IV* were marked with *unc-24*(*e138*) and all the worms were grown under conditions described previously [20,21].

2.2. cDNA cloning and sequencing

Several cDNA clones covering the gene C33B4.3 were obtained from Y. Kohara (National Institute of Genetics, Japan). The phage suspensions of the cDNA clones were excised in vivo according to the methods previously described [22]. The cDNA inserts contained in the pBluescript II plasmid vector were sequenced using T3 and T7 primers. To obtain the 5′ region up to exon 7 not covered by cDNA clones, primers were designed based on database gene sequence predictions and polymerase chain reaction (PCR) of a mixed stage cDNA library (provided by P. Okkema and A. Fire) was performed to obtain

*Corresponding author. Fax: (82)-62-970 2484.
E-mail address: joohong@kjist.ac.kr (J. Ahnn).

0014-5793/04/$30.00
doi:10.1016/S0014-5793(04)00107-3

two independent cDNA fragments. An upstream primer (5′-GATGAATCAAGAGGAGGACACCGTTA) and a downstream primer (5′-GCAGACATTGGACCTTTTCGTACACT) were used to amplify a fragment of 1167 bp and another upstream primer (5′-GTTCGATGTCCCAATCCTCAATATGC) and downstream primer (5′-GGTGGTTCTGATGATTCTGATGTTGC) were used to amplify a cDNA fragment of 1128 bp. These fragments were subcloned into pGEM-T Easy vector (Promega) and confirmed by sequencing.

2.3. Construction of green fluorescent protein (GFP) reporter gene fusion and expression analysis

For pCH105, a 4775-bp fragment containing the 5′ upstream promoter region and part of exon 1 of *shn-1* was amplified from cosmid C33B4 (provided by A. Coulson, Sanger Center, UK) and subcloned into the pPD95.75 vector (provided by A. Fire, Carnegie Institution of Washington, USA) using *Pst*I and *Bam*HI restriction enzyme sites. In order to construct pCH107, a 5657-bp fragment containing the entire coding sequence of *shn-1* was amplified from cosmid C33B4 and was inserted in-frame into pCH105 using *Bam*HI and *Sma*I restriction enzyme sites. The pCH107 construct contains a 4.7-kb 5′ upstream promoter region and the complete *shn-1* coding sequence. The resulting pCH105 and pCH107 constructs were microinjected according to Mello and Fire [23] by co-injecting with pRF4 vector which causes a dominant mutant *rol-6* phenotype as a transformation marker [24]. Animals from subsequent generations were immobilized on a 2% agarose pad by 1 mM levamisole treatment and analyzed for GFP expression patterns under a fluorescent microscope (Olympus BX50) with Nomarski optics.

2.4. Antibodies, immunofluorescence and immunogold staining

Anti-rat Shank1 rabbit polyclonal Shank antibody (1115) was generated using as immunogen a His_6 fusion protein containing amino acids 1–411 of rat Shank1, the region containing the ankyrin repeats containing region. Affinity purification of anti-Shank antibodies was performed using the same fusion proteins immobilized on polyvinylidene difluoride membranes. Wild-type *C. elegans* was immunostained as previously described [25,26]. Animals were permeabilized by freeze-cracking, fixed in cold methanol, and stained with anti-rat Shank1 antibody (1115) and rhodamine-conjugated goat anti-rabbit IgG secondary antibody. Slides were mounted and observed under a fluorescent microscope.

Immunogold staining of adult N2 worms was carried out as described [27]. Specimens were incubated for 2 h at room temperature with anti-rat Shank1 antibody (1115). Following a thorough wash in

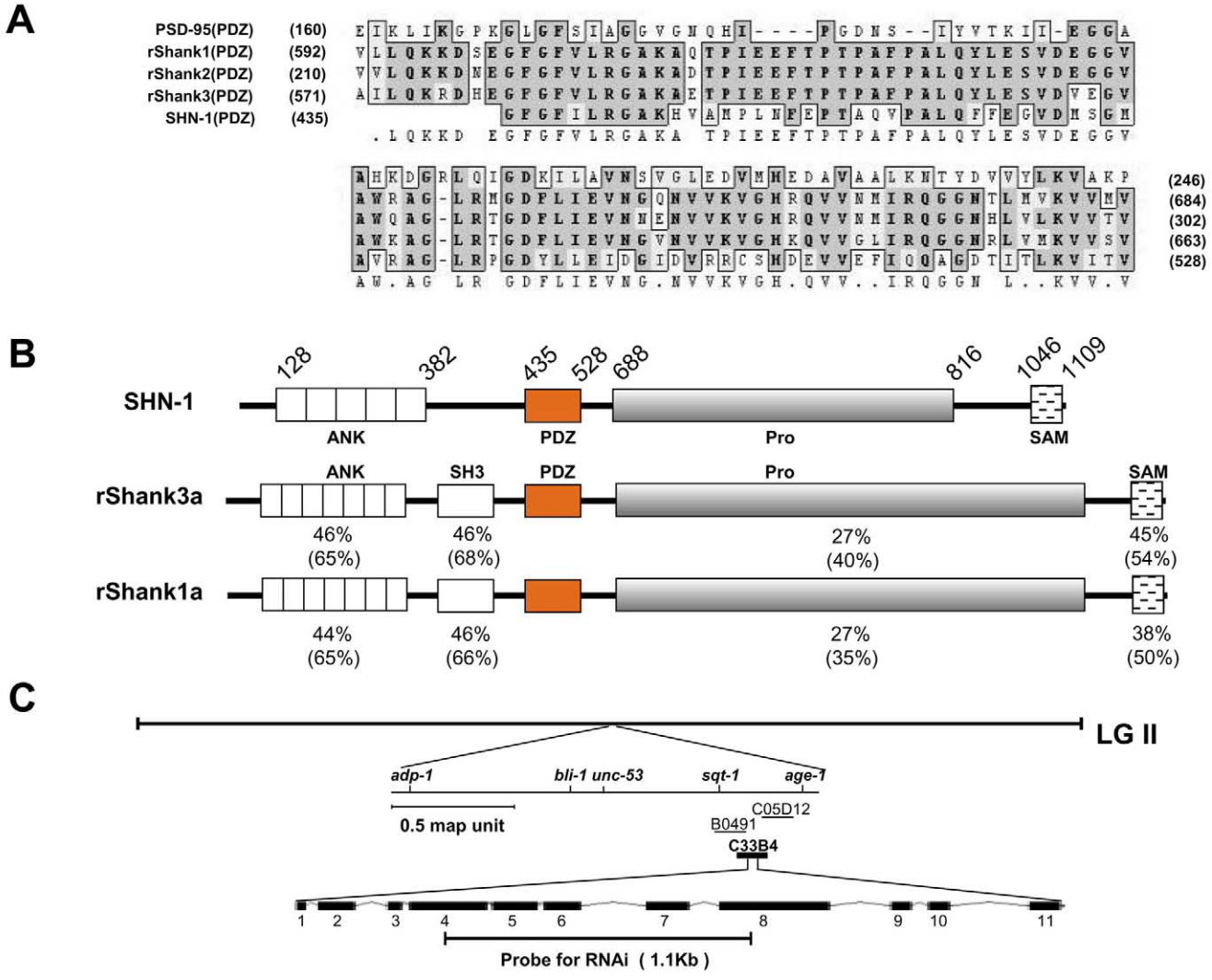

Fig. 1. Identification of SHN-1 in *C. elegans*. A: Amino acid alignment of the PDZ domain of *C. elegans* SHN-1 with PSD-95 and three Shank isoforms of rat. Both identical and similar sequences are boxed and identical sequences are in bold. B: Domain structure of SHN-1, rat Shank1a, and rat Shank3a depicting the ankyrin repeats (ANK), the SH3 (Src homology) domain, the PDZ domain, the proline-rich domain (Pro) and the SAM domain. Percentages below the domains indicate the respective identity and (in parentheses) similarity in comparison to SHN-1. C: Physical and genetic map of the *shn-1* locus and *shn-1* gene structure. The region used in RNAi is indicated below the genomic structure.

PBS-BT (1% bovine serum albumin and 0.01% Tween 20 in phosphate-buffered saline), the specimens were re-incubated overnight at 4°C with 5 nm gold-conjugated goat anti-rabbit IgG antibody (Bio-Cell). For silver enhancement, a commercial kit was used (Amersham) and the background was stained with uranyl acetate and lead citrate. Samples were air-dried and examined under a transmission electron microscope (Jeol 1200 EXII).

2.5. RNA-mediated interference and defecation analysis

A 1128-bp cDNA fragment obtained by PCR amplification (see Section 2.2) was transcribed in vitro using a kit (Promega) and double-stranded RNA was prepared as described [28]. dsRNA injections (1 μg/μl) were carried out in the body cavity of L3 and young adult N2, *itr-1*(*sy290*)*unc-24*(*e138*), *itr-1*(*sy331*)*unc-24*(*e138*), *itr-1*(*sy328*)*unc-24*(*e138*), and *itr-1*(*sa73*) hermaphrodites as described [28]. After 18 h of recovery on bacteria-seeded NGM agar plates, the injected worms were transferred to fresh NGM plates at 24-h intervals. The progeny of injected animals were observed for phenotypes. The experiment was repeated three times [N2 ($n = 30$), buffer- and RNA-injected *itr-1*(*sy290*) ($n = 30$), buffer- and RNA-injected *itr-1*(*sy331*) ($n = 30$), buffer- and RNA-injected *itr-1*(*sy328*) ($n = 30$), buffer-injected *itr-1(sa73)* ($n = 40$), RNA-injected *itr-1(sa73)* ($n = 45$)]. Defecation cycles of indi-

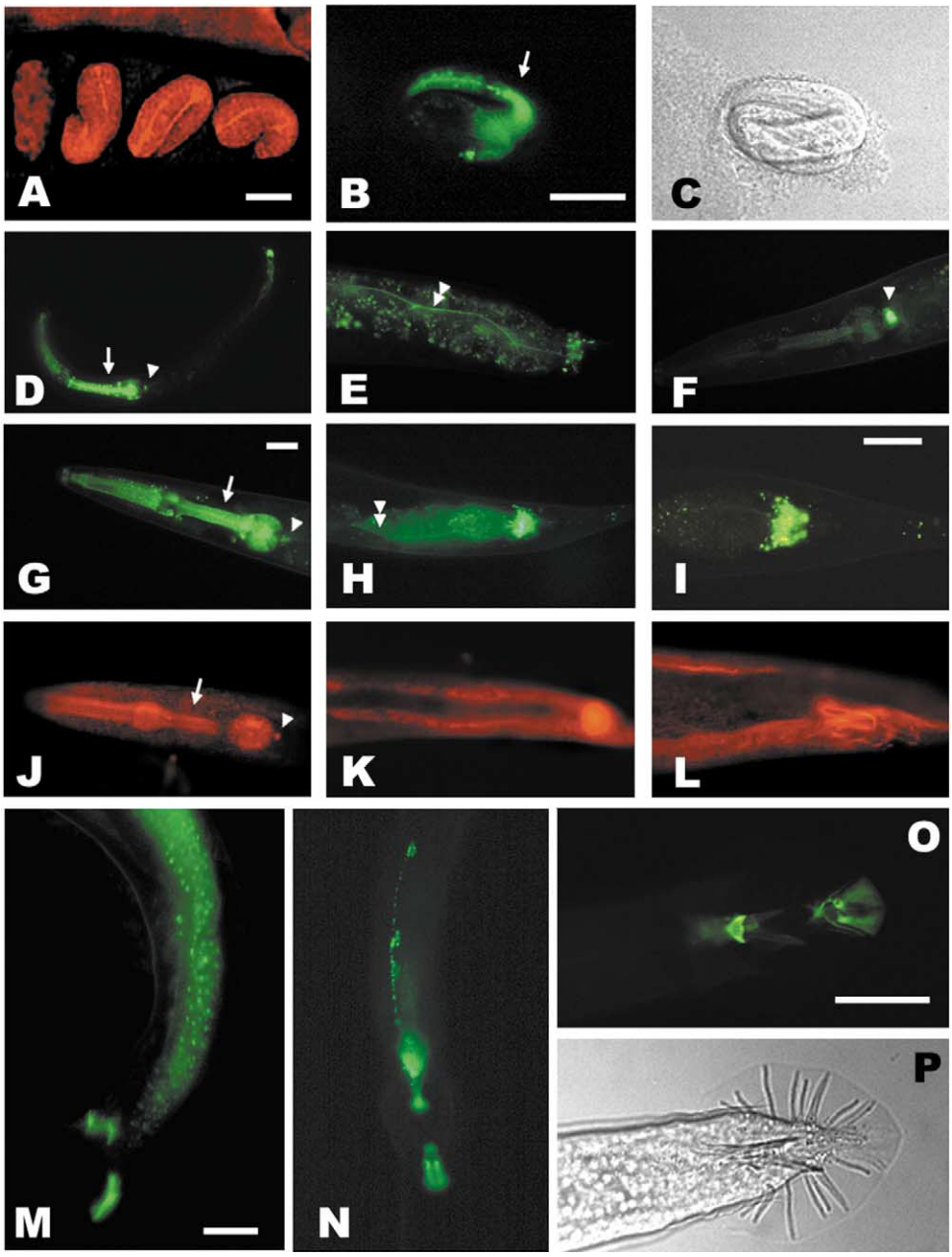

Fig. 2. Expression and localization of SHN-1. The *shn-1* gene containing 4.7-kb of 5′ upstream DNA sequence and complete coding sequence was fused with GFP using pPD95.75 reporter plasmid (pCH107). The transgenic worms were observed under a fluorescence microscope (B,D–I,M,N,O) or with differential interference contrast (DIC) optics (C,P). SHN-1::GFP expressed from embryo to adult (B: embryo, D: L2 larvae, E–I: adult) in pharynx (arrow), pharyngeal-intestinal valve (arrowhead), ventral nerve cord (double arrowhead), intestine (E,H,I,M), rectal epithelial cells (H,I) and male tail (M,N,O). D shows pharyngeal and posterior intestinal expression of shn-1 in L2 larvae and M–O show expression in adult male. Wild-type *C. elegans* were immunostained with primary anti-rat Shank1 polyclonal antibodies (1115) and rhodamine-conjugated secondary antibody. Signals were detected from embryo to adult stage worms (A,J,K,L). Wild-type worms showed strong signal in developing nerve cords of embryos (A), in pharynx (arrow), pharyngeal-intestinal valve (arrowhead), intestine (K), rectal epithelial cells (rep) and tail neurons of adult stage worms (K,L). Each scale bar represents 20 μm.

vidual progeny were scored under a dissecting microscope as described [29]. In brief, mid-L4 stage F1 progenies from dsRNA-injected worms were individually cloned into a single plate. After 36 h, each plate was briefly taken from the 20°C incubator and defecation was measured in an air-conditioned small room. The room temperature was adjusted at 22°C for both RNAi and defecation analysis.

3. Results

3.1. *Identification of a putative Shank homologue in* C. elegans

We have searched the *C. elegans* genome database to identify a Shank homologue in *C. elegans*. In contrast to mam-

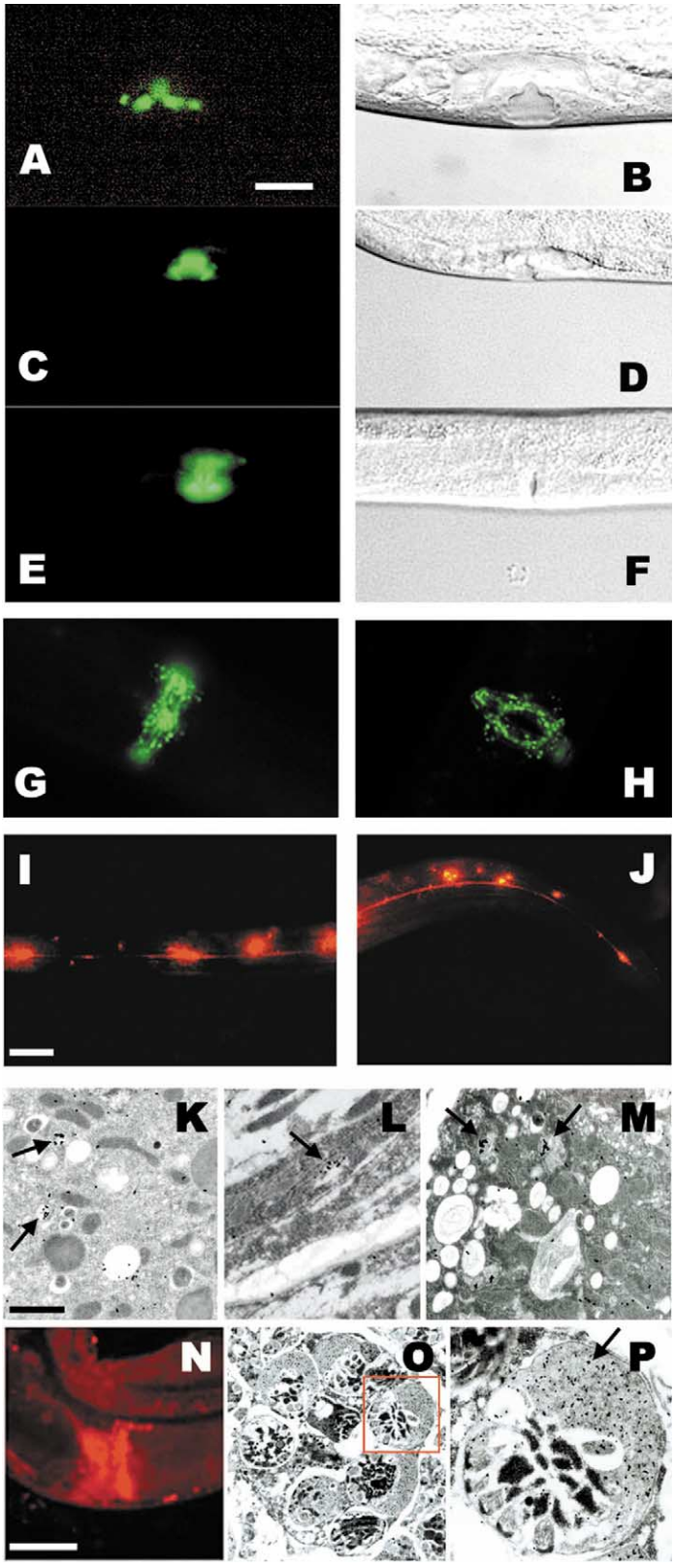

mals, which have at least three isoforms of Shank, only one putative Shank homologue, designated *shn-1*, was found in the *C. elegans* genome. The *shn-1* gene product shows approximately 40% identity over 1000 amino acid residues compared to both rat Shank1 and rat Shank3, and shows higher sequence identity in the regions of ankyrin repeats (ANK), the PDZ (PSD-95, Dlg, and ZO-1) domain, and the SAM domain (Fig. 1A,B).

The full-length cDNA clone was constructed using available cDNA clones covering the C-terminal region of *shn-1* and by PCR amplification of the N-terminal region from the cDNA library. Sequencing these clones confirmed the full-length open reading frame. The *shn-1* gene consists of 11 exons encoding 1110 amino acids and is located at the center of linkage group II between the *sqt-1* and *age-1* loci (Fig. 1C).

3.2. shn-1 *is expressed in neurons, pharynx, intestine, vulva, and sperm*

Since mammalian forms of Shank are known to be expressed mostly in neurons, we sought to examine the expression pattern of SHN-1 in *C. elegans*. The *shn-1* promoter-driven GFP constructs containing 4.8 kb of *shn-1* upstream sequences and the complete genomic sequences of *shn-1* were injected into worms to generate transgenic animals. SHN-1::GFP is expressed in neurons including nerve cords, pharynx, pharyngeal-intestinal valve, intestine, vulva, rectal epithelial cells and tail ganglia (Figs. 2 and 3).

We also analyzed Shank protein localization by whole-mount immunostaining with anti-rat Shank1 antibody (1115) that is specific for Shank1 protein. Immunostaining revealed that endogenous SHN-1 protein is expressed from the embryonic stage to adulthood (Fig. 2A,J–L) and tissue localization overlapped with SHN-1::GFP expression patterns in the pharynx, pharyngeal-intestinal valve, intestine, nerve cords, and tail region in addition to sperm (Figs. 2 and 3).

To study the subcellular localization of SHN-1 in further detail, we conducted immunogold electron microscopy in wild-type hermaphrodites and males. Signals were detected in the vesicle-like structures of intestinal and pharyngeal cells, and in the tail region (Fig. 3K–M), and most clearly seen in the male germline in developing sperm and in the presumptive pseudopodia, structures for motility of mature sperm (Fig. 3O,P). Further confirmation of SHN-1 localization might be needed in order to implicate it in the function of these tissues.

3.3. *SHN-1 affects defecation rhythm via* itr-1*, which encodes an IP$_3$ receptor homologue*

Double-stranded RNAi is an effective method to inhibit gene function in *C. elegans* [28]. Thus, we injected *shn-1* dsRNA into wild-type animals to analyze possible functions of *C. elegans* Shank at the organism level. However, no obvious phenotypes were observed in these animals. We then conducted immunostaining of the progenies of injected worms to determine the tissue-specific interference effect of *shn-1* RNAi. As shown in Fig. 3I,J, RNA-affected worms displayed residual staining only in neuronal tissues indicating that potent suppression of SHN-1 occurred in several tissues including intestine and pharynx. We assessed the condition of the RNAi worms and concluded that there were no obvious effects on embryonic lethality, growth, and morphology, though we observed a slight, statistically insignificant reduction in brood size (data not shown). Thus, the loss of *shn-1* in non-neuronal tissue does not lead to severe abnormalities in *C. elegans*.

Although no obvious abnormalities were observed, we suspected more subtle defects could be found in RNAi worms deficient in *shn-1*. The expression pattern of *shn-1* was very similar to that of *itr-1*, the IP$_3$ receptor gene in *C. elegans* [29,30], which regulates the defecation cycle in *C. elegans*. Previous genetic studies reported that a loss-of-function mutation in *itr-1*(*sa73*) causes much longer defecation times ([29] and Fig. 4B). Therefore, we assessed the RNAi effect on defecation cycles, an ultradian rhythmic behavior generated and controlled by intestinal cells independently of neuronal mechanisms [29,31], in both wild-type and RNAi-treated worms. The defecation cycle comprises three consecutive body muscle contractions that recur approximately every 50 s to mediate expulsion of waste. Defecation cycle is quantified by measuring the duration from one of the three muscle contractions, that of the posterior body wall muscle (pBoc), to the next pBoc contraction. *C. elegans* subjected to SHN-1 RNAi showed normal defecation behavior (average was 43.2 s and coefficient of variation (CV = S.D./mean × 100) was 6.6) compared to buffer-injected wild-type worms (average was 42.8 s and CV was 6.5), indicating that loss of SHN-1 alone was not sufficient to affect defecation cycles.

It has been shown that the rhythmic defecation cycle is regulated by the periodic release of calcium from the endoplasmic reticulum mediated by the IP$_3$ receptor [29]. Mutations in *itr-1*, which encodes the IP$_3$ receptor in *C. elegans*, slow down the defecation cycle significantly ([29] and Fig. 4B). Since Shank is also known to be involved in the synaptic recruitment of IP$_3$ receptors to regulate dendritic spine morphology [19], we tested whether SHN-1 is required for ITR-1 function in control of defecation cycle. We injected dsRNA targeted for *shn-1* into both *itr-1* loss-of-function and gain-of-function mutants. Intriguingly, loss-of-function mutant *itr-*

←

Fig. 3. Tissue and cellular localization of SHN-1 stained by anti-rat Shank1 polyclonal antibody and vulval expression. GFP expression controlled by 5′-upstream region of *shn-1* gene (pCH105) was observed in vulval epithelial cells of an L4 hermaphrodite (A,C,E) during vulval induction and DIC images (B,D,F) are shown. G and H show expression pattern in vulval epithelial cells caused by the pCH107 construct, which contained the 5′-upstream region and complete coding sequence. F1 progenies of dsRNA-injected *C. elegans* (I,J) were immunostained with primary anti-rat Shank1 polyclonal antibodies (1115) and rhodamine-conjugated secondary antibody. In RNA-treated animals, signals in pharynx and intestine disappeared, but expression in neurons remained strong in the anterior (I) and posterior (J) regions of the worm. I shows the anterior region of RNAi-treated worms, J the posterior region. Each scale bar represents 20 μm. Subcellular localization of SHN-1 in intestine (K), pharynx (L), male tail (M) and sperm (O,P). Gold particles were found aggregated in vesicle-like structures (arrow) of transverse section of intestine (K), and sections through pharynx (L) and male tail (M) showing specific localization of SHN-1. SHN-1 signals were detected in the spermatheca by immunostaining (N) and the localization was specifically confirmed in sperm by immunogold electron microscopy (O,P). The boxed area in O containing one sperm is magnified in P. SHN-1 is clearly localized in the presumptive pseudopodium (arrow indicate general region) in P. Each scale bar represents 0.5 μm.

1(*sa73*) treated with RNAi showed a much longer defecation cycle (average 146.8 s) than control animals (average 93.1 s) (Fig. 4C). Variability also increased significantly when compared to both the wild-type worms and the *itr-1*(*sa73*) mutants not treated with RNAi (Fig. 4A,B) indicating that normal consistent defecation patterns have been disrupted. More interestingly, the gain-of-function mutants of *itr-1* [(*sy290*), (*sy331*), and (*sy328*)] treated with *shn-1* RNAi showed virtually no differences in defecation cycle compared to control animals. These data suggest a possible interaction between

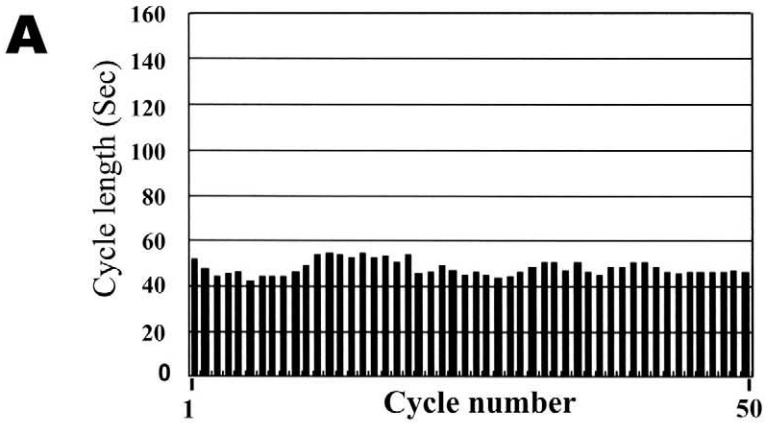

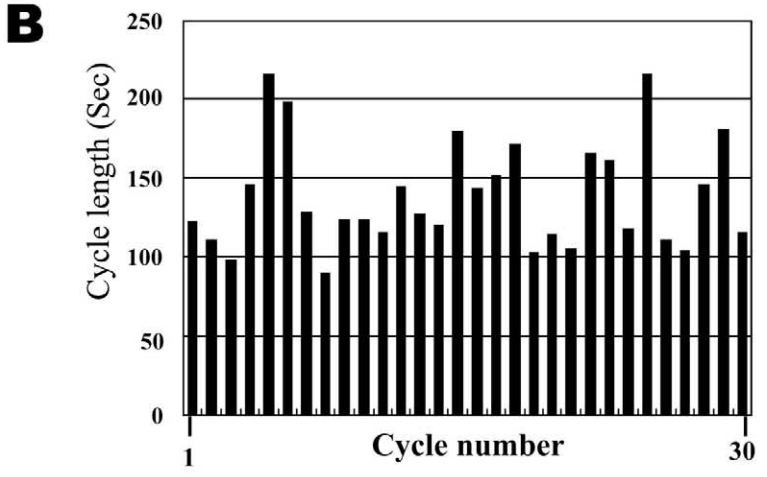

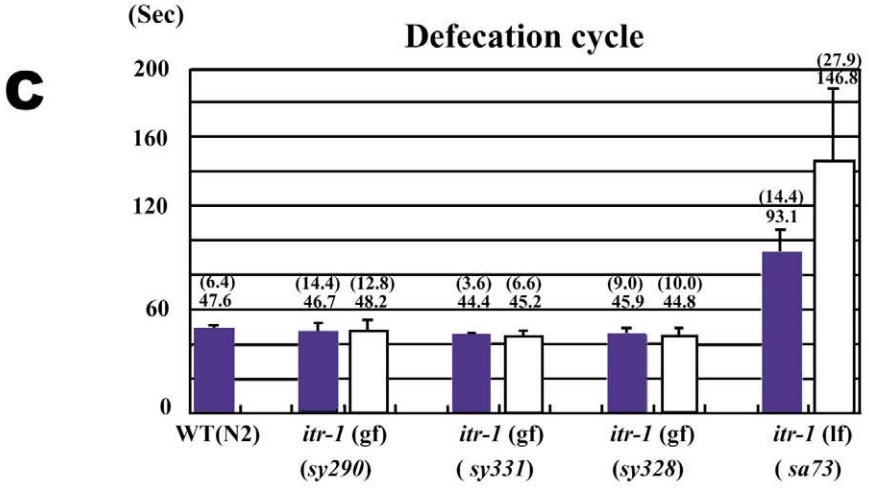

the *shn-1* and *itr-1* genes, which could be tested if mutants of *shn-1* become available. Based on our results and the known function of Shank as a scaffold recruiting IP_3 receptor in other systems we might speculate that Shank is important for recruiting IP_3 receptors to regulate the defecation cycle in *C. elegans*.

4. Discussion

We have identified and characterized *shn-1*, the *C. elegans* homologue of Shank, which is known to be a scaffolding protein. Although it remains to be determined whether the PSD exists in *C. elegans*, the appropriate localization of proteins to polarized membranes is important in simple, multicellular organisms like the nematodes. Scaffolding functions such as those proteins involved in the localization of the LET-23 receptor in vulva epithelial cells have been shown to be conserved with different roles in mammalian neurons [32]. Therefore, it is quite possible that the roles that SHN-1 may fulfill as a scaffolding protein in non-neuronal polarized cells may also be conserved in the PSDs of neurons in higher organisms. Thus, *C. elegans*, with its conserved and convenient genetic composition, is an excellent model for studies of scaffolding proteins.

We analyzed Shank expression and localization in *C. elegans* by GFP analysis, whole-mount immunostaining, and immunogold electron microscopy. Staining pattern by anti-rat Shank1 antibody, whose specificity to *C. elegans* Shank was verified by Western blot analysis (data not shown), not only confirms GFP expression results but also shows the conservation of Shank protein. Localization of SHN-1 was not confirmed to neuronal tissues as observed in Shank1 [11]; instead, it is expressed in diverse polarized cell types including sperm, epithelial, and intestinal cells, a pattern more similar to that exhibited by Shank3 [11]. More specifically, SHN-1 signals were concentrated in the pseudopodia of spermatids. This suggests that SHN-1 may play a role in sperm motility. Shank is known to regulate the growth and morphology of dendritic spines, which uses actin-based motility to extend the dendritic portion of neurons into a 'mushroom' shape upon which synapses can form [19,33]. Although nematode sperm movement via pseudopodia is not actin-based [34], a role for Shank in sperm crawling involving MSP, which fulfills a role analogous to actin [35], is a possibility.

Although most of the known roles of Shank in mammalian cells involve neuronal functions, we were unable to find any roles of SHN-1 in neuronal tissue due to the lack of RNAi effect in *C. elegans* neurons. Thus, we sought to identify functions in other tissues that could be revealed by RNAi. We found that loss of SHN-1 in intestinal cells of the *itr-1*(*sa73 lf*) mutant conferred longer and variable defecation cycles, suggesting a genetic and possible biochemical relationship between these two proteins consistent with previous reports that Shank recruits IP_3 receptors during mammalian dendritic spine formation [19]. This is also supported by similar expression patterns of both *shn-1* and *itr-1* in the intestine, and also in the pharynx, pharyngeal-intestinal valve, and vulva epithelial cells [29,30], whereas there are no known Homer homologues in the *C. elegans* genome.

What purpose could IP_3 receptor localization via Shank serve in intestinal cells for the maintenance of the defecation cycle? Two possibilities exist: the first one requires IP_3 receptor localization for the production of a polarized IP_3 signal in the cytosol, while the second possibility involves a polarized calcium efflux from the endoplasmic reticulum that makes proper IP_3 receptor localization necessary. Interestingly, a recent study showed that disruption of IP_3 signaling by using a transgenic IP_3 binding region as an IP_3 'sponge' results in defecation phenotypes with longer and more variable cycles [37] similar to defects observed in Shank RNAi in *itr-1*(*sa73*) loss-of-function mutants (Fig. 4B,C). These data together with our data support the possibility that the defecation rhythm is directly correlated with IP_3 concentration and the ability of the IP_3 receptor to effectively receive and bind the IP_3 signal by proper receptor localization rather than calcium response of the IP_3 receptor itself.

This idea may also explain the RNAi result in gain-of-function *itr-1* mutant [(*sy290*), (*sy331*), and (*sy328*)] backgrounds. Surprisingly, there was no difference in defecation cycles when RNAi was administered to these gain-of function mutants, which have mutations in the IP_3 binding region [36]. It is possible that these receptors with gain-of-function mutations require less restricted localization, so that RNAi for *shn-1* would fail to affect defecation cycles in these mutants. Taken together, our data show that proper localization of shank may play an important role in the maintenance of the ultradian defecation rhythm.

We have described the evolutionary conservation of the PSD scaffolding protein Shank at the gene, protein, and functional level in *C. elegans*. The conserved relationship between Shank and the IP_3 receptor evidenced by genetic interaction in *C. elegans* suggests that these two proteins not only function together at the cellular level but also may be involved in complex mechanisms that affect the entire organism. Since this genetic interaction has its limitations, further molecular characterization of the nature of this interaction is needed. As the first examination of Shank function at the organism level, *shn-1* in *C. elegans* should provide some insight for future studies in other multicellular organisms.

Acknowledgements: The authors would like to thank A. Coulson for the cosmids, Y. Kohara for cDNA clones, the CGC for worm strains, B.K. Dhakal for manuscript preparation. This work was supported by Grant 1999-2-21000-001-3 from KOSEF, BK21, and Korean Systems Biology Research Grant M1-0309-00-006 from the Korea Ministry of Science and Technology.

←

Fig. 4. Disruption of SHN-1 in *itr-1*(*sa73*) mutants affects the length and periodic behavior of defecation cycles. Length of defecation cycle is measured as the time between consecutive contractions of the posterior body wall muscle (pBoc). A: A record of sequential defecation cycle periods in a wild-type animal. Variations in cycle length are minimal due to the rhythmic behavior. B: A record of sequential defecation cycle periods in a *shn-1* RNAi-affected *itr-1*(*sa73*) mutant. Large fluctuations from cycle to cycle indicate a disruption in the rhythmic behavior. C: Average length of defecation cycles in wild-type, *itr-1* mutant, and *shn-1* RNAi-affected *itr-1* mutant worms. White bars indicate *shn-1* RNAi-affected worms of the indicated *itr-1* mutant strain. The numbers above the bars show average defecation time in seconds and the numbers in parentheses represent coefficients of variation (CV = S.D./mean × 100). The large error bar in *shn-1* RNAi-affected *itr-1*(*sa73*) mutant worms is indicative of the irregular defecation rhythm observed in B.

References

[1] Sheng, M. (1996) Neuron 17, 575–578.
[2] Kornau, H., Seeburg, P. and Kennedy, M. (1997) Curr. Opin. Neurobiol. 7, 368–373.
[3] Ziff, E.B. (1997) Neuron 19, 1163–1174.
[4] Craven, S. and Bredt, D. (1998) Cell 15, 495–498.
[5] Dong, H., O'Brien, R.J., Fung, E.T., Lanahan, A.A., Worley, P.F. and Huganir, R.L. (1997) Nature 386, 279–284.
[6] O'Brien, R., Lau, L. and Huganir, R. (1998) Curr. Opin. Neurobiol. 8, 364–369.
[7] Wyszynski, M., Kim, E., Yang, F.C. and Sheng, M. (1998) Neuropharmacology 37, 1335–1344.
[8] Xiao, B., Tu, J.C., Petralia, R.S., Yuan, J.P., Doan, A., Breder, C.D., Ruggiero, A., Lanahan, A.A., Wenthold, R.J. and Worley, P.F. (1998) Neuron 21, 707–716.
[9] Naisbitt, S., Kim, E., Tu, J.C., Xiao, B., Sala, C., Valtschanoff, J., Weinberg, R.J., Worley, P.F. and Sheng, M. (1999) Neuron 23, 569–582.
[10] Sheng, M. and Kim, E. (2000) J. Cell Sci. 113, 1851–1856.
[11] Lim, S., Naisbitt, S., Yoon, J., Hwang, J.I., Suh, P.G., Sheng, M. and Kim, E. (1999) J. Biol. Chem. 274, 29510–29518.
[12] Boeckers, T.M., Kreutz, M.R., Winter, C., Zuschratter, W., Smalla, K.H., Sanmarti-Vila, L., Wex, H., Langnaese, K., Bockmann, J., Garner, C.C. and Gundelfinger, E.D. (1999) J. Neurosci. 19, 6505–6518.
[13] Yao, I., Hata, Y., Hirao, K., Deguchi, M., Ide, N., Takeuchi, M. and Takai, Y. (1999) J. Biol. Chem. 274, 27463–27466.
[14] Zitzer, H., Honck, H.H., Bachner, D., Richter, D. and Kreienkamp, H.J. (1999) J. Biol. Chem. 274, 32997–33001.
[15] Du, Y., Weed, S.A., Xiong, W.C., Marshall, T.D. and Parsons, J.T. (1998) Mol. Cell. Biol. 18, 5838–5851.
[16] Tu, J.C., Xiao, B., Naisbitt, S., Yuan, J.P., Petralia, R.S., Brakeman, P., Doan, A., Aakalu, V.K., Lanahan, A.A., Sheng, M. and Worley, P.F. (1999) Neuron 23, 583–592.
[17] Wu, H. and Parsons, J.T. (1993) J. Cell Biol. 120, 1417–1426.
[18] Tu, J.C., Xiao, B., Yuan, J.P., Lanahan, A.A., Leoffert, K., Li, M., Linden, D.J. and Worley, P.F. (1998) Neuron 21, 717–726.
[19] Sala, C., Plech, V., Wilson, N.R., Passafaro, M., Liu, G. and Sheng, M. (2001) Neuron 31, 115–130.
[20] Brenner, S. (1974) Genetics 77, 71–94.
[21] Sulston, J. and Hodgkin, J. (1988) in: The Nematode *Caenorhabditis elegans* (Wood, W.B., Ed.), pp. 585–607, Cold Spring Harbor Laboratory Press, Cold Spring Harbor, NY.
[22] Sambrook, J., Fritsch, E.F. and Maniatis, T. (1989) Molecular Cloning: A Laboratory Manual, Cold Spring Harbor Laboratory Press, Cold Spring Harbor, NY.
[23] Mello, C. and Fire, A. (1995) Methods Cell Biol. 48, 451–482.
[24] Krammer, J., French, R.P., Park, E. and Johnson, J.J. (1990) Mol. Cell. Biol. 10, 2981–2990.
[25] Miller, D.M. and Shakes, D.C. (1995) Methods Cell Biol. 48, 365–394.
[26] Cho, J.H., Oh, Y.S., Park, K.W., Yu, J., Choi, K.Y., Shin, J., Kim, D.H., Park, W.J., Hamada, T., Kagawa, H., Maryon, E.B., Bandyopadhyay, J. and Ahnn, J. (2000) J. Cell Sci. 113, 3947–3958.
[27] Yu, J.R. and Chai, J.Y. (1995) Korean J. Parasitol. 3, 155–164.
[28] Fire, A., Xu, S., Montgomery, M.K., Kostas, S.A., Driver, S.E. and Mello, C. (1998) Nature 391, 806–811.
[29] Dal Santo, P., Logan, M.A., Chisholm, A.D. and Jorgensen, E.M. (1999) Cell 98, 757–767.
[30] Gower, N.J., Temple, G.R., Schein, J.E., Marra, M., Walker, D.S. and Baylis, H.A. (2001) J. Mol. Biol. 306, 145–157.
[31] Liu, D.W. and Thomas, J.H. (1994) J. Neurosci. 14, 1953–1962.
[32] Setou, M., Nakagawa, T., Seog, D.H. and Hirokawa, N. (2000) Science 288, 1796–1802.
[33] Fischer, M., Kaech, S., Knutti, D. and Matus, A. (1998) Neuron 20, 847–854.
[34] Roberts, T.M. and Streitmatter, G. (1984) J. Cell Sci. 69, 117–126.
[35] Miller, M.A., Nguyen, V.Q., Lee, M.H., Kosinski, M., Schedl, T., Caprioli, R.M. and Greenstein, D. (2001) Science 291, 2144–2147.
[36] Clandinin, T.R., DeModena, J.A. and Sternberg, P.W. (1998) Cell 92, 523–533.
[37] Walker, D.S., Gower, N.J.D., Ly, S., Bradley, G. and Baylis, H.A. (2002) Mol. Biol. Cell 13, 1329–1337.